Molecular Neurobiology (2019) 56:3563–3575
https://doi.org/10.1007/s12035-018-1319-y

Astrocytic Mechanisms Involving Kynurenic Acid Control Δ^9-Tetrahydrocannabinol-Induced Increases in Glutamate Release in Brain Reward-Processing Areas

Maria E. Secci[1] · Paola Mascia[1] · Claudia Sagheddu[2] · Sarah Beggiato[3,4] · Miriam Melis[2] · Andrea C. Borelli[5] · Maria C. Tomasini[4] · Leigh V. Panlilio[1] · Charles W. Schindler[1] · Gianluigi Tanda[6] · Sergi Ferré[6] · Charles W. Bradberry[1] · Luca Ferraro[4] · Marco Pistis[2,7] · Steven R. Goldberg[1] · Robert Schwarcz[3] · Zuzana Justinova[1]

Received: 2 May 2018 / Accepted: 14 August 2018 / Published online: 27 August 2018

Abstract

The reinforcing effects of Δ^9-tetrahydrocannabinol (THC) in rats and monkeys, and the reinforcement-related dopamine-releasing effects of THC in rats, can be attenuated by increasing endogenous levels of kynurenic acid (KYNA) through systemic administration of the kynurenine 3-monooxygenase inhibitor, Ro 61-8048. KYNA is a negative allosteric modulator of α7 nicotinic acetylcholine receptors (α7nAChRs) and is synthesized and released by astroglia, which express functional α7nAChRs and cannabinoid CB1 receptors (CB1Rs). Here, we tested whether these presumed KYNA autoreceptors (α7nAChRs) and CB1Rs regulate glutamate release. We used in vivo microdialysis and electrophysiology in rats, RNAscope in situ hybridization in brain slices, and primary culture of rat cortical astrocytes. Acute systemic administration of THC increased extracellular levels of glutamate in the nucleus accumbens shell (NAcS), ventral tegmental area (VTA), and medial prefrontal cortex (mPFC). THC also reduced extracellular levels of KYNA in the NAcS. These THC effects were prevented by administration of Ro 61-8048 or the CB1R antagonist, rimonabant. THC increased the firing activity of glutamatergic pyramidal neurons projecting from the mPFC to the NAcS or to the VTA in vivo. These effects were averted by pretreatment with Ro 61-8048. In vitro, THC elicited glutamate release from cortical astrocytes (on which we demonstrated co-localization of the CB1Rs and α7nAChR mRNAs), and this effect was prevented by KYNA and rimonabant. These results suggest a key role of astrocytes in interactions between the endocannabinoid system, kynurenine pathway, and glutamatergic neurotransmission, with ramifications for the pathophysiology and treatment of psychiatric and neurodegenerative diseases.

Keywords Astrocytes · Cannabinoids · Glutamate · Kynurenic acid · Rat · THC

Maria E. Secci, Paola Mascia, Claudia Sagheddu and Sarah Beggiato contributed equally to this work.

Steven R. Goldberg is deceased. This paper is dedicated to his memory.

Electronic supplementary material The online version of this article (https://doi.org/10.1007/s12035-018-1319-y) contains supplementary material, which is available to authorized users.

✉ Zuzana Justinova
zuzana.justinova@nih.gov

[1] Behavioral Neuroscience Research Branch, Intramural Research Program, Department of Health and Human Services, National Institute on Drug Abuse, National Institutes of Health, 251 Bayview Blvd., Baltimore, MD 21224, USA

[2] Department of Biomedical Sciences, University of Cagliari, Monserrato, Italy

[3] Maryland Psychiatric Research Center, Department of Psychiatry, University of Maryland School of Medicine, Baltimore, MD, USA

[4] Department of Life Sciences and Biotechnology, University of Ferrara, Ferrara, Italy

[5] Department of Medical Sciences, University of Ferrara, Ferrara, Italy

[6] Molecular Targets and Medications Discovery Branch, Intramural Research Program, Department of Health and Human Services, National Institute on Drug Abuse, National Institutes of Health, Baltimore, MD, USA

[7] National Research Council of Italy (CNR), Section of Cagliari, Neuroscience Institute, Monserrato, Italy

Background

Cannabis, one of the most widely abused drugs in the USA [1], can produce adverse effects including memory impairment and panic attacks, and has been associated with an enhanced incidence of psychosis [2–4]. Chronic use can lead to dependence and cannabis use disorder, and discontinuation of chronic use can produce withdrawal symptoms such as anxiety, insomnia, and depressed mood (DSM-5) [5]. The mechanisms involved in the reinforcing and addictive effects of cannabis are not as well understood as those of opioids or psychostimulant drugs [6, 7].

Δ^9-Tetrahydrocannabinol (THC), the primary psychoactive ingredient in marijuana and other cannabis preparations, increases the activity of mesolimbic dopamine neurons by stimulating cannabinoid CB1 receptors (CB1Rs) [8, 9]. This effect is widely believed to be central to the drug's psychoactive properties, but significant ambiguity remains regarding the magnitude of the effect and inconsistency between findings from animal and human studies [10]. Cannabinoids also affect glutamatergic neurotransmission [11–15]. For example, acute administration of THC raises the extracellular levels of glutamate in the rat prefrontal cortex in vivo [16], and administration of the synthetic CB1/CB2R agonist WIN 55,212-2 increases extracellular glutamate in primary cultures of rat prefrontal cortical neurons [17]. As glutamate can stimulate mesencephalic or striatal dopamine release by activating glutamate receptors on dopaminergic neuronal dendrites and terminals [18–20], these and other studies suggest that glutamate may, in fact, play a critical intermediary role in the THC-induced increase in dopaminergic neurotransmission [10, 21, 22].

The relationship between THC and glutamate may involve astrocytes, which express functional CB1Rs [23, 24]. Activation of these receptors promotes the release of glutamate [25], which, in turn—and in line with the concept of the tripartite synapse—modulates neuronal excitability [26–29]. Moreover, recent evidence suggests the active participation of kynurenic acid (KYNA), a neuroactive metabolite of the kynurenine pathway of tryptophan degradation, which is synthesized in and released from astrocytes and has multiple links to glutamatergic neurotransmission [30]. In the mammalian brain, endogenous KYNA, at concentrations in the nanomolar range, acts predominantly as a negative allosteric modulator of α7 nicotinic acetylcholine receptors (α7nAChRs) [31–33], which are present both on glutamatergic nerve terminals and on astrocytes and can thus modulate glutamate release [18, 20, 34–37]. Notably, as α7nAChR inhibition by KYNA depends on several factors including cell maturation, neuronal type, and receptor location (dendrite vs. soma), some experimental approaches fail to corroborate the physiological relevance of this phenomenon [38–41] (see Albuquerque and Schwarcz [42] for review). Although KYNA can also inhibit the obligatory glycine$_B$ site of the NMDA receptor [43], this effect does not appear to influence glutamate release since administration of the more potent, selective NMDA/glycine$_B$ receptor antagonist 7-chlorokynurenic acid does not reduce extracellular glutamate levels in vivo [44].

Inhibition of kynurenine 3-monooxygenase (KMO), a key enzyme for the conversion of kynurenine into the neurotoxin quinolinic acid, shifts kynurenine pathway metabolism toward enhanced KYNA formation [30]. Systemic administration of the KMO inhibitor Ro 61-8048 increases KYNA levels in the nucleus accumbens shell (NAcS) and the ventral tegmental area (VTA) in rats [45]. Notably, even relatively small increases in KYNA concentrations in the brain reduce cannabinoid-induced dopamine release in reward-associated brain areas (NAcS, VTA) and block THC self-administration and relapse-like reinstatement of THC-seeking behavior in squirrel monkeys [45]. This suggested that enhancement of brain KYNA levels might be exploited for the development of medications to treat cannabinoid dependence. Interactions between kynurenine and endocannabinoids also have possible therapeutic relevance for other pathological conditions, such as psychosis, migraine, and epilepsy, though the mechanisms involved might differ between distinct pathological states [46].

Using complementary neurochemical and electrophysiological methodologies in vivo and in vitro, the present study was designed to examine the relationship between THC, glutamate, and KYNA. Our results provide evidence for an involvement of both glutamate and KYNA in the effects of THC in reward-associated areas of the brain and suggest that astrocytic CB1Rs and α7nAChRs may play key roles in these events.

Materials and Methods

Animals

Male Sprague-Dawley rats (Charles River Laboratories, Wilmington, MA, USA, or Envigo RMS, San Pietro Natisone, Udine, Italy), weighing 300–350 g, were pair-housed. Adult pregnant Sprague-Dawley rats (gestational age: 2 days) were obtained from Charles River Laboratories, Calco (Lecco), Italy. All animals were maintained in temperature- and humidity-controlled facilities. Animals were kept on a 12-h/12-h light/dark cycle (lights on from 7:00 a.m.) and had ad libitum access to food and water. All experiments were conducted during the light phase.

Drugs

For microdialysis experiments, THC (NIDA Drug Supply Program, Rockville, MD, USA) was dissolved in 40% (*w*/*v*) cyclodextrin in saline. For in vivo electrophysiology studies, THC, obtained in a 20% (*v*/*v*) ethanol solution (THC PHARM GmbH, Frankfurt, Germany), was emulsified in 1% (*v*/*v*) Tween 80, diluted in saline. The kynurenine 3-monooxygenase (KMO) inhibitor Ro 61-8048 (3,4-dimethoxy-*N*-[4-(3-nitrophenyl)thiazol-2-yl]benzenesulfonamide, Sai Advantium Pharma, Hyderabad, India) was dissolved in vehicle containing 5–6% (*v*/*v*) Tween 80 in saline and was administered 40 min before THC. Rimonabant (5-(4-chlorophenyl)-1-(2,4-dichloro-phenyl)-4-methyl-*N*-(piperidin-1-yl)-1H-pyrazole-3-carboxamide, SR141716A, NIDA Drug Supply Program, Rockville, MD, USA) was dissolved in a vehicle containing 2% (*v*/*v*) Tween 80, 2% (*v*/*v*) ethanol, and sterile water and was administered 40 min before THC.

For use in primary astrocyte cultures, the commercially obtained THC solution (1 mg in 1 ml methanol; Sigma-Aldrich) was diluted in distilled water. The final methanol concentration ranged between 0.0001% (*v*/*v*) and 0.03% (*v*/*v*). WIN 55,212-2, KYNA and rimonabant were purchased from Tocris (Milano, Italy) and dissolved in dimethyl sulfoxide (DMSO) and distilled water. The final concentration of DMSO was < 0.01%.

Dulbecco's modified Eagle's medium (DMEM), fetal bovine serum (FBS), and phosphate-buffered saline (PBS) solution were purchased from Gibco, Thermo-Fischer Scientific (Monza, Italy). Penicillin, streptomycin, poly-L-lysine, and Triton X-100 were obtained from Sigma-Aldrich (Milan, Italy). Anti-glial fibrillary acidic protein (GFAP) antibodies were purchased from Chemicon (Temecula, CA, USA).

In Vivo Microdialysis in Freely Moving Rats

As previously described [47, 48], microdialysis was performed 20–24 h after the implantation of probes in the medial prefrontal cortex (mPFC; AP: + 3.5 mm from bregma, L: ± 0.5 from the midline, V: − 5.0 mm from the dura), the shell of the NAcS (AP: + 2.0 mm, L: ± 1.1 mm, V: − 8.0 mm), or the VTA (AP: − 5.3 mm, L: ± 0.9 mm, V: − 8.4 mm) [49], at a perfusion rate of 1 μl/min (probe length: NAcS 2 mm, VTA 1 mm, mPFC 4 mm; hand-crafted in the lab). Samples were collected every 20 min, rapidly frozen, and stored at − 80 °C until the day of analysis. Only data from rats with correct probe placement were included in the study ($n = 123$). Brains were harvested at the end of the experiments and cut on a cryostat in consecutive coronal slices (40 μm) to confirm probe placement. Intraperitoneal (i.p.) injections of Ro 61-8048 (30 or 100 mg/kg), rimonabant (1 mg/kg), or the respective vehicles were made 40 min prior to the injection of THC (3 mg/kg, i.p.). The timelines of the experiments are shown in Figs. 1a and 2a. Analysis of glutamate and KYNA is described in detail in "Supplementary Methods."

In Vivo Electrophysiology

Surgery and recordings were performed as described previously [50] ($n = 44$). Details are published in "Supplementary Methods."

Single-unit activity of PFC neurons (AP: 3.0 mm from bregma, L: ± 0.8–1.0 mm from the midline) located in layers III–VI (V: 1.0–3.5 mm from the cortical surface) was recorded. Electrophysiological characteristics of the recorded cells corresponded to those attributed to pyramidal neurons [51, 52]. They presented "regular-spiking" or "intrinsically bursting" activity, the firing rate never exceeded 10 Hz, and the action potentials were > 2 ms wide. PFC output neurons were identified by antidromic spikes, elicited by VTA (AP: − 6.0 mm from bregma, L: ± 0.5 mm from the midline; V: 7.5 mm from the cortical surface) or NAcS (AP: 1.0 mm from bregma; L: ± 1.0 mm from the midline; V: 7.4 mm from the cortical surface; 20° AP inclination) stimulation.

Single-unit activity of neurons located in the VTA (AP: − 6.0 mm from bregma; L: ± 0.4–0.6 mm from the midline; V: 7.0–8.0 mm from the cortical surface) was recorded extracellularly (bandpass filter 0.1–10,000 Hz). Dopamine neurons were isolated and identified according to published criteria [3, 53–55], i.e., a firing rate < 10 Hz and > 2.5 ms duration of the action potential. Bursts were defined as the occurrence of two spikes at an interspike interval of < 80 ms and terminated when the interspike interval exceeded 160 ms. VTA-NAcS output neurons were identified by antidromic spikes elicited by NAcS stimulation (AP: 1.5 mm from bregma, L: ± 1.0 mm from the midline, V: 7 mm from the cortical surface) on the basis that they were of fixed latency and collided with spontaneous spikes.

RNAscope In Situ Hybridization Assay

RNA in situ hybridization (ISH) was performed for Cnr1, Rn-Chrna7, and GFAP. Rats were decapitated ($n = 5$), and the brain was rapidly removed and frozen in isopentane (kept on dry ice) for 15 s before being transferred to a sealed bag for long-term storage at − 80 °C. After equilibrating the tissue in a cryostat (Leica CM 3050S) at − 20 °C for 2 h, 10-μm brain slices of the mPFC were collected at approximately + 3.2 mm from bregma [49] and mounted directly onto Super Frost Plus slides (Fisher Scientific, Cat. no. 12-550-15). The slides were left at − 20 °C for 1 h and then stored at − 80 °C. For ISH, a RNAscope Multiplex Fluorescent Reagent Kit (Advanced Cell Diagnostics, Newark, CA, USA) was used according to the user manual for fresh frozen tissue. Details of the procedures are described in "Supplementary Methods."

Primary Cultures of Cortical Astrocytes

Primary cultures of cortical astrocytes were obtained from rats on embryonic day 18 ($n = 32$; 4 dams, 8 fetuses from each)

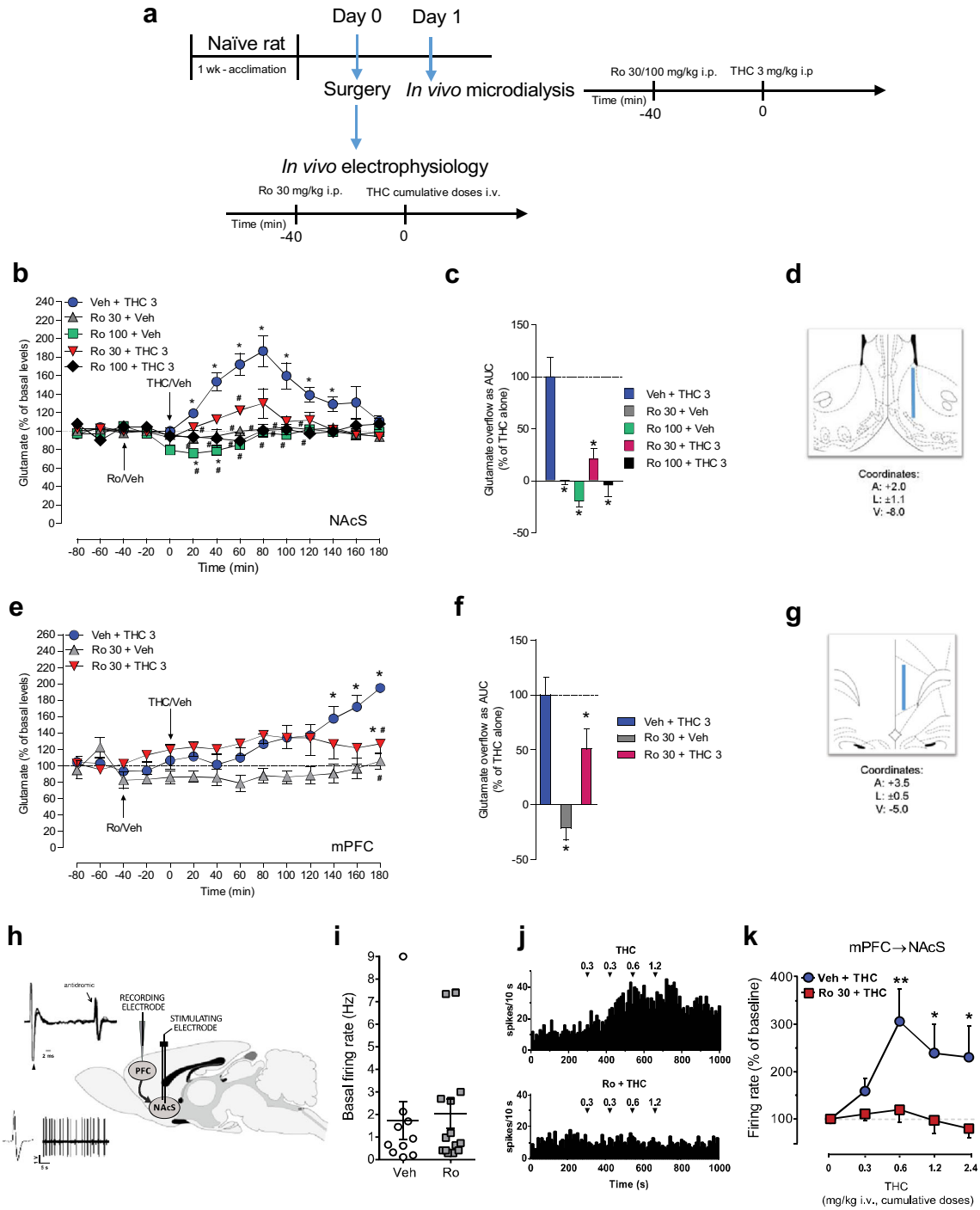

and cultured as described previously [56], with slight modifications detailed in "Supplementary Methods."

Endogenous Extracellular Glutamate Levels

On the day of the experiment, cells were rinsed twice (1 min/rinse) by replacing the culture medium with a warmed (37 °C) Krebs-Ringer bicarbonate buffer (mM: NaCl 118.5, KCl 4.8, $CaCl_2$ 2.5, $MgSO_4$ 1.2, $NaHCO_3$ 25, NaH_2PO_4 1.2, glucose 11; pH 7.4). Thereafter, 200 µl of Krebs-Ringer bicarbonate buffer was added, and the solution was maintained for 40 min. Subsequently, 100 µl was collected, and the remaining Krebs-Ringer buffer (300 µl) was discharged. This procedure was then repeated to collect a total of four consecutive fractions. The mean of the first two fractions was used to define basal endogenous glutamate levels. THC and KYNA were applied 15 and 40 min, respectively, before the end of the third period. When indicated, the CB1R antagonist

◀ **Fig. 1** Effects of the KMO inhibitor Ro 61-8048 on THC-induced changes in the NAcS and in mPFC pyramidal neurons projecting to the NAcS. **a** Timeline of the microdialysis and electrophysiology experiments. **b** Ro 61-8048 (30 or 100 mg/kg, i.p.) reduces the increases in extracellular glutamate levels induced by THC (3 mg/kg, i.p.) in the NAcS. Results are expressed as a percentage of basal glutamate levels over time (Veh + THC 3, $n = 9$; Ro 30 + Veh, $n = 7$; Ro 100 + Veh, $n = 7$; THC 3 + Ro 30, $n = 5$; THC 3 + Ro 100, $n = 7$). $^{*}p < 0.05$ vs. baseline, $^{\#}p < 0.05$ vs. Veh + THC 3. **c** Glutamate levels are expressed as area under the curve (AUC) over the 180 min following THC or Veh injection; $^{*}p < 0.05$ vs. Veh + THC 3. **d** Representation of the probe placement in the NAcS following the Paxinos and Watson brain atlas. **e** Ro 61-8048 (30 mg/kg) reduces the increases in extracellular glutamate levels induced by THC (3 mg/kg, i.p.) in mPFC. Ro 61-8048 alone does not significantly affect glutamate levels in mPFC. Results are expressed as a percentage of basal glutamate levels over time (Veh + THC 3, $n = 5$; Ro 30 + Veh, $n = 5$; THC 3 + Ro 30, $n = 7$). $^{*}p < 0.05$ vs. baseline, $^{\#}p < 0.05$ vs. Veh + THC. **f** Glutamate levels are expressed as the area under the curve (AUC) over the 180 min following THC or Veh injection; $^{*}p < 0.05$ vs. Veh + THC 3. **g** Representation of the probe placement in the mPFC. **h** Diagram representing stimulation (NAcS) and recording (mPFC) areas for in vivo electrophysiology experiments. Traces illustrate representative extracellular recordings of mPFC pyramidal neurons. Identification of the antidromic response induced by the electrical stimulation of the NAcS in mPFC cell: digital storage oscilloscope traces display fixed latency of the antidromic response. **i** Pretreatment with Ro 61-8048 (30 mg/kg, i.p.) does not change basal firing activity of mPFC pyramidal neurons projecting to NAcS (unpaired *t* test). **j** Representative firing rate histograms of mPFC → NAcS neurons from rats pretreated with Veh (top) or Ro 61-8048 (30 mg/kg, i.p.; bottom) prior to cumulative THC injections (0.3–1.2 mg/kg, i.v.). **k** Ro 61-8048 abolishes the THC-induced increase in firing activity of mPFC pyramidal neurons projecting to the NAcS (Veh + THC, $n = 6$; Ro + THC, $n = 6$), $^{*}p < 0.05$, $^{**}p<0.01$, two-way ANOVA and Bonferroni test. Symbols and bars represent means ± SEM in **b**, **c**, **e**, **f**, and **k**. Arrows indicate time of injections (**b**, **e**, **j**). Veh = vehicle, Ro = Ro 61-8048

rimonabant was added 20 min before THC. Pharmacological agents were not present during the fourth collection period (see Fig. 4f for a schematic representation of the experimental design). The effects of the treatments on endogenous extracellular glutamate levels were expressed as a percentage of basal values.

In this study, glutamate was quantified using a modified HPLC method [17], involving pre-column derivatization. To this end, *o*-phthalaldehyde/β-mercaptoethanol (1:1, *v*/*v*) was added to each sample, and 25 μl was then applied to a reverse-phase HPLC column (Chromsep 5 C_{18} column 5 μm; 100 × 3 mm, Superchrom, Milan, Italy). The mobile phase (flow rate: 0.75 ml/min) consisted of 0.1 M sodium acetate, 10% methanol, and 2.5% tetrahydrofuran, pH 6.5. In the eluate, glutamate was detected fluorimetrically (Shimadzu RF-551, Tokyo, Japan), using excitation and emission wavelengths of 370 and 450 nm, respectively. The retention time of glutamate was approximately 3.5 min. The limit of detection (LOD) was 30 fmoles. Validation parameters are described in the "Supplementary Methods."

Statistical Analyses

In vivo microdialysis data were not adjusted for recovery from the dialysis probe. Basal values were calculated as the mean of three consecutive samples (differing by no more than 15%) collected immediately preceding the drug treatment. Data were expressed as a percentage of basal values and were analyzed using one-way ANOVA or two-way mixed analysis (with treatment as a fixed effect and time as a repeated measure) using Proc Mixed (SAS Institute, Cary, NC, USA). When appropriate, post hoc analysis was performed using Tukey's multiple comparisons test.

For in vivo electrophysiology, drug-induced changes in firing rate and regularity were calculated by averaging the effects of the drugs for the 2-min period following drug administration and comparing them to the mean of the pre-drug baseline. Statistical significance was assessed using two-way ANOVA for repeated measures, or one-way ANOVA, or Student's *t* test when appropriate, using GraphPad Prism5. Post hoc multiple comparisons were made using the Bonferroni correction.

Data obtained from astrocyte cultures were analyzed using GraphPad Prism5. Statistical analysis was carried out by ANOVA followed by the Newman-Keuls test for multiple comparisons.

The assumptions of statistical tests used in the analyses were verified by examining residuals for deviations from normality. All results are expressed as means ± S.E.M. $p < 0.05$ was the accepted level of significance in all experiments.

Results

Effects of Ro 61-8048 on THC-Induced Changes in Extracellular Glutamate Levels in the NAcS and in the mPFC

Basal levels of extracellular glutamate in the NAcS were 0.73 ± 0.05 μM. Administration of 3 mg/kg of THC (i.p.), a dose known to elevate extracellular levels of dopamine in reward-associated brain areas in rats [57], significantly increased extracellular glutamate, with a maximal effect observed after 80 min (Fig. 1b; treatment × time interaction: $F(36,257) = 3.58$, $p < 0.01$). Pretreatment with 30 or 100 mg/kg of Ro 61-8048 dose-dependently counteracted the glutamate-releasing effects of THC (Fig. 1b). When given alone, Ro 61-8048 did not affect glutamate levels in the NAcS at a dose of 30 mg/kg, whereas 100 mg/kg produced a modest reduction in extracellular glutamate 60 and 80 min after administration of the KMO inhibitor (Fig. 1b). Figure 1c illustrates the calculated areas under the curves (AUC; $F(4,30) = 16.39$, $p < 0.01$), and Fig. 1d illustrates the probe placement in the NAcS.

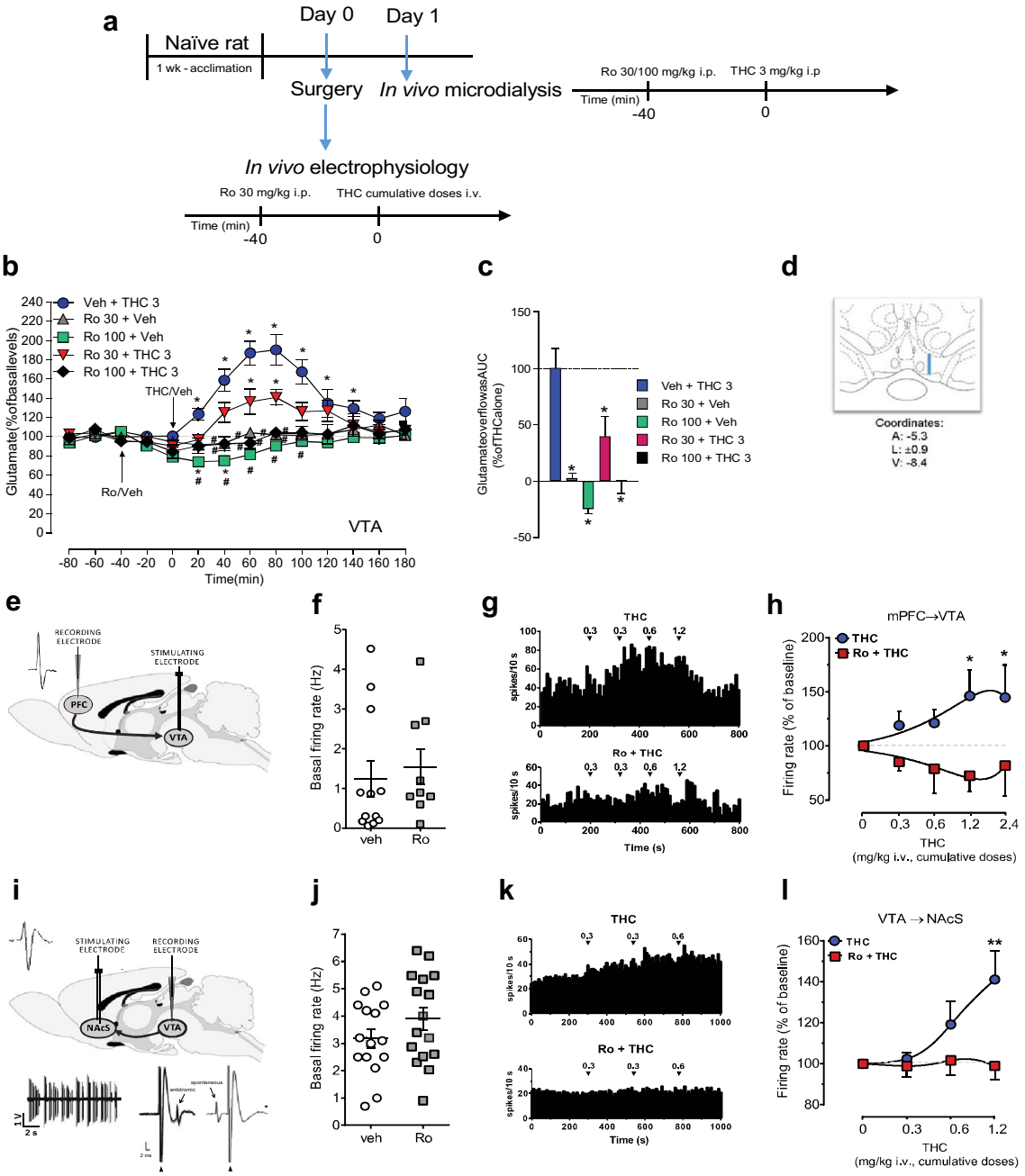

Fig. 2 Effects of Ro 61-8048 on THC-induced changes in the VTA and in mPFC pyramidal neurons projecting to the VTA, and in dopaminergic cell projecting from the VTA to the NAcS. **a** Timeline of the microdialysis and electrophysiology experiments. **b** Ro 61-8048 (30 or 100 mg/kg, i.p.) reduces the increases in extracellular glutamate levels produced by THC (3 mg/kg, i.p.) in the VTA. Results are expressed as a percentage of basal glutamate levels over time (Veh + THC 3, $n = 10$; Ro 30 + Veh, $n = 8$; Ro 100 + Veh, $n = 6$; THC 3 + Ro 30, $n = 5$; THC 3 + Ro 100, $n = 6$). $^{*}p < 0.05$ vs. baseline, $^{\#}p < 0.05$ vs. Veh + THC 3. **c** Glutamate levels are expressed as area under the curve (AUC) over the 180 min following THC or Veh injection; $^{*}p < 0.05$ vs. Veh + THC 3. **d** Representation of the probe placement in the NAcS following the Paxinos and Watson brain atlas. **e** Diagram representing stimulation (VTA) and recording (mPFC) areas for in vivo electrophysiology experiments. **f** Pretreatment with Ro 61-8048 does not change basal firing activity of mPFC pyramidal neurons projecting to the VTA (unpaired *t* test). **g** Representative firing rate histograms of mPFC → VTA neurons from rats pretreated with Veh (top) or Ro 61-8048 (30 mg/kg, i.p.; bottom) prior to cumulative THC (0.3–1.2 mg/kg) i.v. injections. **h** Pretreatment with Ro 61-8048 abolished THC-induced increase in firing activity of mPFC pyramidal neurons projecting to the VTA (Veh + THC, $n = 6$; Ro + THC, $n = 5$), $^{*}p < 0.05$, two-way ANOVA and Bonferroni test. **i** Diagram representing stimulation (NAcS) and recording (VTA) areas in the rat brain for dopamine neuron in vivo electrophysiology recordings. **j** Pretreatment with Ro 61-8048 does not change basal firing activity of mPFC pyramidal neurons projecting to VTA (unpaired *t* test). **k** Representative firing rate histograms of dopamine VTA → NAcS neurons from rats pretreated with Veh (top) or Ro 61-8048 (30 mg/kg, i.p.; bottom) prior to cumulative THC injections (0.3–0.6 mg/kg, i.v.). **l** Pretreatment with Ro 61-8048 abolishes THC-induced increase in firing activity of dopamine cells projecting to the NAcS (Veh + THC, $n = 12$; Ro + THC, $n = 9$), $^{**}p < 0.01$, two-way ANOVA and Bonferroni test. Symbols and bars represent means ± SEM in **b**, **c**, **h**, and **l**. Arrows indicate time of injections (**b**, **g**, **k**). Veh = vehicle, Ro = Ro 61-8048

Basal levels of extracellular glutamate in the mPFC were 1.75 ± 0.36 μM. In agreement with the study of Pistis and colleagues [16], which had reported an increase in extracellular glutamate levels in the PFC following an i.v. application of THC (1 mg/kg), i.p. administration of THC (3 mg/kg) significantly increased extracellular glutamate levels (Fig. 1e; effect of group: $F(2,13) = 7.92$, $p < 0.01$; effect of time: $F(9,117) = 3.02$, $p < 0.01$; Fig. 1f; AUC: $F(2,13) = 7.42$, $p < 0.01$). In contrast to the NAcS (Fig. 1b), however, statistical significance of this effect was not reached until 140 min after the THC injection, and glutamate levels continued to rise up to 180 min. Pretreatment with 30 mg/kg of Ro 61-8048 prevented the THC-induced effect on extracellular glutamate at the 180 min time point (Fig. 1e, f). When applied alone, Ro 61-8048 (30 mg/kg) did not influence glutamate levels in the mPFC (Fig. 1e, f). Figure 1g illustrates the probe placement in the mPFC.

Effects of Ro 61-8048 on THC-Induced Changes in the Firing Rate of mPFC → NAcS Neurons

Based on the biochemical data described above, we next examined the effects of THC on mPFC cells that were antidromically identified as output neurons projecting to the NAcS (Fig. 1h) by electrophysiological means. As illustrated in Fig. 1j, k, THC (cumulative 0.3–2.4 mg/kg, i.v.) produced a dose-dependent increase in the firing rate of mPFC → NAcS neurons in vivo (one-way ANOVA for repeated measures, $F(4,20) = 4.44$, $p < 0.05$). This effect was prevented by i.p. pretreatment with 30 mg/kg of Ro 61-8048 (repeated measures one-way ANOVA, $F(4,20) = 1.22$, $p < 0.05$; dose-response curves analyzed with two-way ANOVA for repeated measures $F(2,40) = 6.01$, $p < 0.05$), with no changes in the basal firing rate (Fig. 1i; unpaired t test $t_{22} = 0.28$, $p > 0.05$).

THC-Induced Changes in Extracellular Glutamate Levels in the VTA: Effect of Ro 61-8048

Basal levels of extracellular glutamate in the VTA were 0.83 ± 0.05 μM. Administration of 3 mg/kg THC (i.p.) significantly increased the extracellular levels of glutamate (Fig. 2b; treatment × time interaction, $F(36,269) = 3.81$, $p < 0.01$; Fig. 2c; AUC: $F(4,31) = 16.22$, $p < 0.01$). As in the NAcS (Fig. 1b), the maximal effect was observed after 80 min. Pretreatment with 30 or 100 mg/kg of Ro 61-8048 (i.p.) dose-dependently prevented this effect of THC (Fig. 2b, c). Only the higher dose of Ro 61-8048 (100 mg/kg) significantly decreased basal extracellular glutamate levels 40–100 min after administration (Fig. 2b, c). Figure 2d illustrates the probe placement in the VTA.

Effects of Ro 61-8048 on THC-Induced Changes in the Firing Rate of mPFC → VTA and VTA → NAcS Neurons

To examine the physiological significance of the microdialysis results illustrated in Fig. 2b, c, we studied efferents from the mPFC to the VTA (Fig. 2e) and efferents from the VTA to the NAcS (Fig. 2i) electrophysiologically. Cumulative i.v. administration of THC (0.3–2.4 and 0.3–1.2 mg/kg, respectively) dose-dependently increased the firing rate of both projection neurons (Fig. 2g, h, k, l). Pretreatment with 30 mg/kg of Ro 61-8048 abolished the THC-induced increases in firing rate of mPFC neurons projecting to the VTA (Fig. 2g, h; two-way ANOVA for repeated measures $F(2,44) = 4.04$, $p < 0.05$), without changes in basal activity (Fig. 2f; unpaired t test $t_{21} = 0.55$, $p > 0.05$). The same treatment also prevented the effects of THC on VTA dopamine cells that were antidromically identified as projecting to the NAcS (Fig. 2k, l; two-way ANOVA for repeated measures $F(2,44) = 4.03$, $p < 0.05$). Here, too, pretreatment with Ro 61-8048 did not alter basal firing activity (Fig. 2j; unpaired t test $t_{29} = 1.33$, $p > 0.05$).

Effects of Rimonabant on THC-Induced Changes in the Extracellular Levels of Glutamate and KYNA in the NAcS

In separate rats, we tested the effects of the CB1R antagonist rimonabant on extracellular glutamate and KYNA levels in the NAcS. Confirming the results shown in Fig. 1b, systemic administration of THC (3 mg/kg, i.p.) significantly increased the extracellular concentration of glutamate (basal levels: 1.56 ± 0.06 μM) (Fig. 3a; treatment × time interaction, $F(18,125) = 3.47$, $p < 0.01$; Fig. 3b; AUC: $F(2,14) = 28.41$, $p < 0.01$). Measured in the same microdialysis samples, extracellular concentrations of KYNA were reduced compared to basal levels (2.15 ± 0.07 nM), with a maximal effect observed 80 min after the administration of THC (Fig. 3c; treatment × time interaction, $F(18,144) = 2.26$, $p < 0.01$; Fig. 3d; AUC: $F(2,16) = 18.58$, $p < 0.01$).

Pretreatment with rimonabant (1 mg/kg, i.p.) abolished the THC-induced glutamate overflow but did not alter glutamate levels when given alone (Fig. 3a, b). Pretreatment with rimonabant (1 mg/kg) also prevented the effect of THC on KYNA levels, again without affecting endogenous levels of the metabolite on its own (Fig. 3c, d).

Co-localization of CB1R and α7nAChR mRNA in Rat Cortical Astrocytes

We used an ultrasensitive RNAscope ISH method to detect low densities of CB1R and α7nAChR mRNA expression in rat cortical astrocytes in the mPFC. First, we validated our hybridization method using control probes. The positive

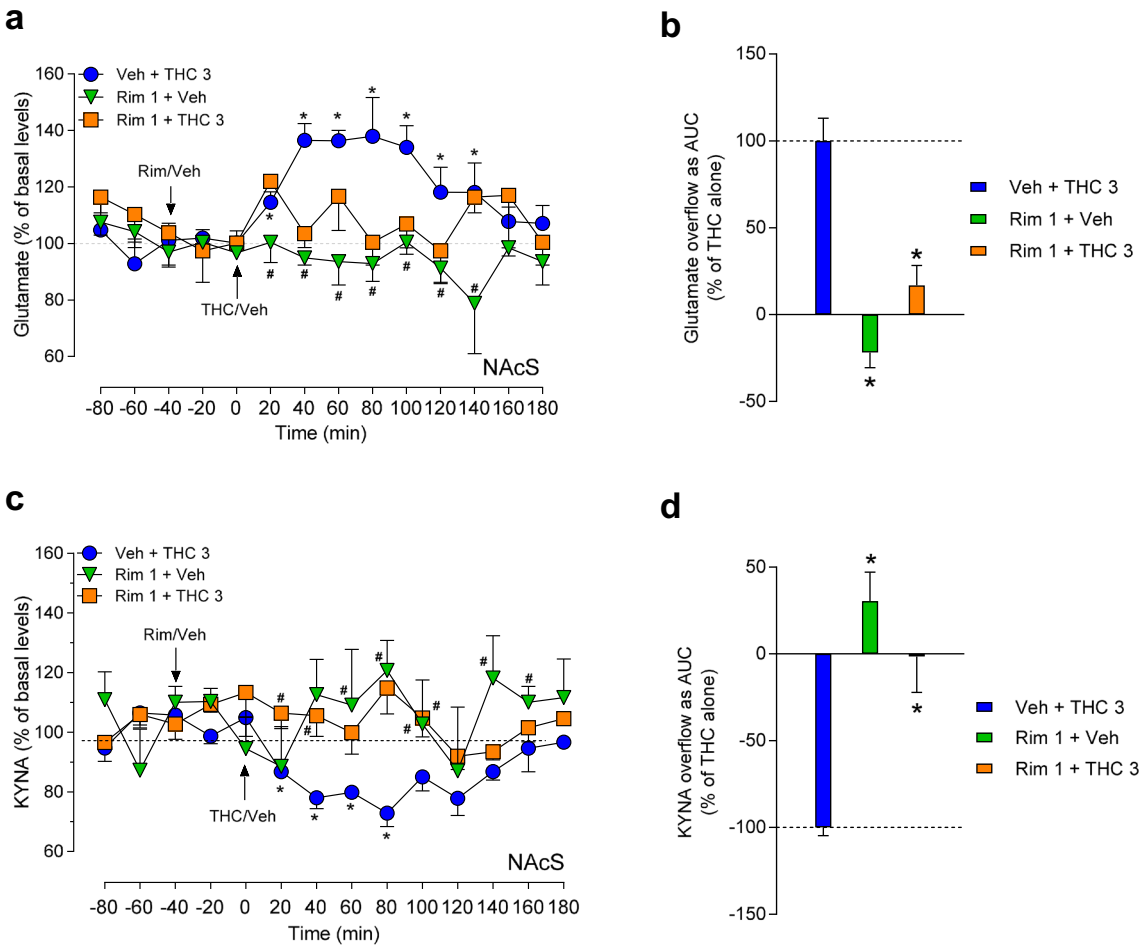

Fig. 3 Effects of rimonabant on THC-induced changes in the extracellular levels of glutamate and KYNA in the NAcS of rats. **a**, **b** Rimonabant (1 mg/kg, i.p.) reduces the increase in extracellular glutamate levels produced by THC (3 mg/kg, i.p.) in the NAcS. **c**, **d** Rimonabant reverses the THC-induced decrease in extracellular KYNA levels in the NAcS. Results are expressed as a percentage of basal glutamate (**a**) or KYNA (**c**) levels over time (**a**, glutamate levels: Veh + THC 3, $n = 6$; Rim 1 + Veh, $n = 5$; Rim 1 + THC 3, $n = 6$; **c**, KYNA levels: Veh + THC 3, $n = 6$; Rim 1 + Veh, $n = 7$; Rim 1 + THC 3, $n = 6$). Arrows indicate time of injection. $^{*}p < 0.05$ vs. baseline, $^{\#}p < 0.05$ vs. Veh + THC 3. Glutamate and KYNA levels are also expressed as areas under the curve (AUC) over the 180 min following THC or Veh injection (**b**, **d**). $^{*}p < 0.05$ vs. Veh + THC 3. Symbols and bars represent means ± SEM. Veh = vehicle. Rim = Rimonabant

controls produced strong fluorescent signals in the mPFC of rats (Fig. 4a; Supplementary Figure S1a–d top panels), whereas the negative control probe generated no fluorescence (Supplementary Figure S1a–d bottom panels). Then, using customized RNAscope probes, we showed the co-existence of both CB1Rs and α7nAChRs in cortical astrocytes. Representative pictures of GFAP/CB1R/α7nAChR triple labeling by RNAscope in situ hybridization are shown in Fig. 4b–e, respectively (top at ×20, bottom at ×63 magnification).

Effects of Rimonabant and KYNA on THC-Induced Extracellular Glutamate Levels in Astrocyte Cultures

Basal extracellular glutamate levels in primary cultures of rat cortical astrocytes were 0.24 ± 0.02 μM and remained essentially stable over the 160-min duration of the experiment (Fig. 4f shows the experimental design, and Fig. 4g shows representative photograph of astrocytes in culture). Addition of 1 μM (but not 30 or 300 nM) THC to the medium during the third collection period significantly ($p < 0.01$) increased extracellular glutamate levels (Fig. 4h). Rimonabant (100 nM), added to the medium 20 min before THC (1 μM), prevented the THC-induced glutamate increase. By itself, rimonabant did not influence extracellular glutamate levels (Fig. 4i). We also analyzed the effects of THC on basal extracellular glutamate levels in the presence of KYNA. Although addition of KYNA (10 nM, 100 nM, or 1 μM) alone did not modify extracellular glutamate (Fig. 4j), KYNA (100 nM) prevented the THC (1 μM)-induced glutamate increase (Fig. 4k). KYNA (10 nM) was ineffective (Fig. 4k).

Similar to THC, WIN 55,212-2 (300 nM and 1 μM) significantly ($p < 0.05$ and $p < 0.01$, respectively) increased basal extracellular glutamate levels. WIN 55,212-2 was ineffective at lower concentrations (1, 10, and 100 nM;

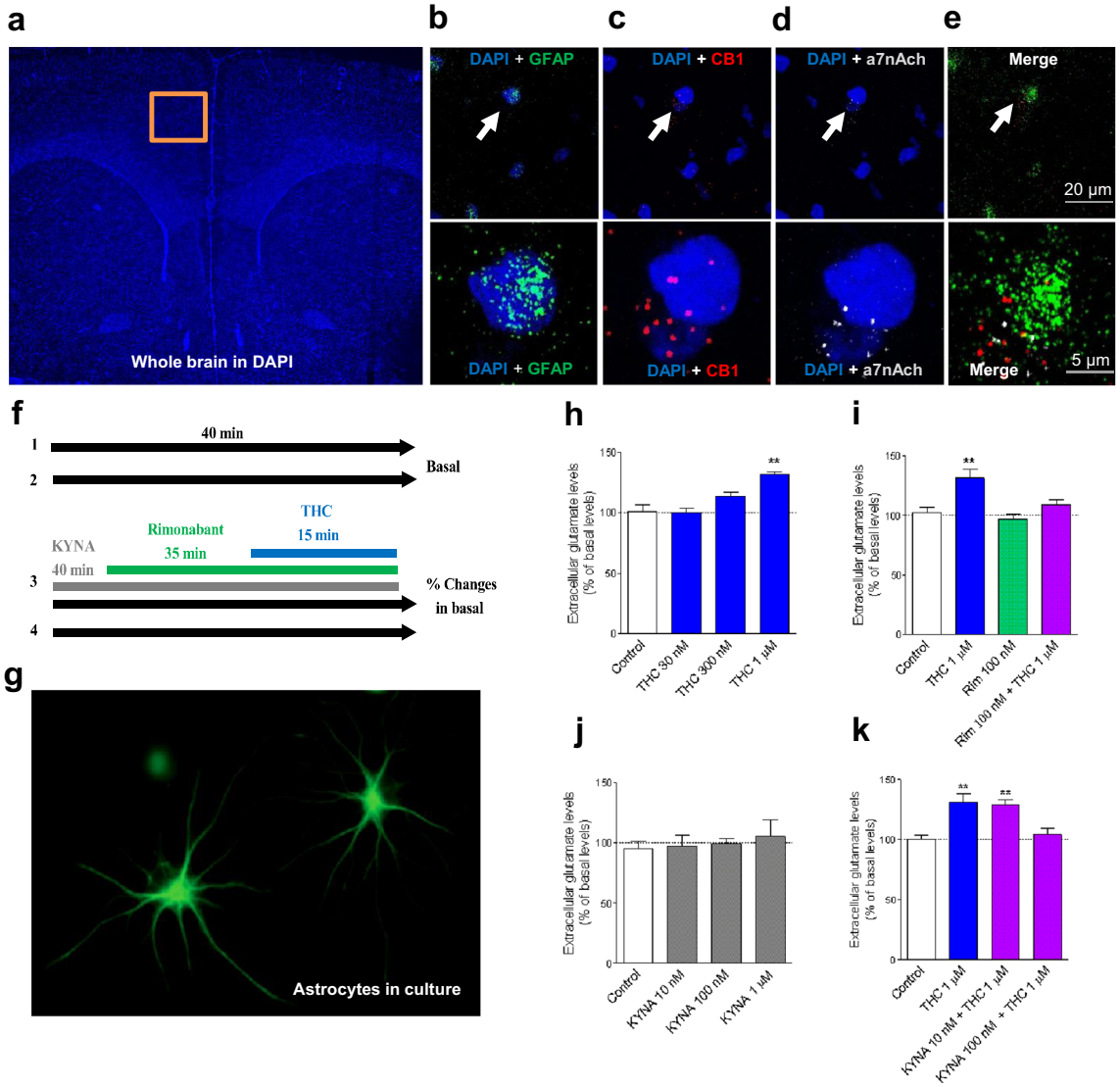

Fig. 4 Expression of CB1Rs and α7nAchRs on rat cortical astrocytes and effects of THC and KYNA on extracellular glutamate levels in primary cultures of rat cortical astrocytes. RNAscope Multiplex Fluorescent Assay was performed on brain slices from adult Sprague-Dawley rats to assess the expression of CB1Rs and α7nAchRs and the results show that both receptors co-localize in GFAP-expressing cells. **a** Representation of the whole brain in DAPI and mPFC target area. **b** (Top) RNAscope for GFAP probes (green); nuclei are stained with DAPI (blue). **b** (Bottom) Magnified image of the cells shown at the top. **c** (Top) RNAscope for CB1R (red) probes; nuclei are stained with DAPI (blue). **c** (Bottom) Magnified image of the cells shown at the top. **d** (Top) RNAscope for α7nACh receptor (white) probes; nuclei are stained with DAPI (blue). **d** (Bottom) Magnified image of the cells shown at the top. **e** (Top) Multiplex RNAscope for GFAP, CB1Rs, and α7nAChRs showing co-localization (merge). **e** (Bottom) Magnified image of the cells shown at the top. **f** Design of experiments using primary cultures of cortical astrocytes: four consecutive fractions were collected every 40 min. THC and KYNA were applied 15 and 40 min, respectively, before the end of the third fraction. Rimonabant was added 35 min before the end of the third fraction (i.e., 20 min before THC). **g** Representative fluorescence photomicrograph of GFAP immunoreactivity: astrocytes were stained with anti-GFAP antibody and observed in sample field under fluorescent microscope (magnification ×40). **h** Effect of THC (30 nM, 300 nM, and 1 μM) on glutamate levels. $^{**}p < 0.01$ significantly different from control, THC 30 and 300 nM. **i** Effect of rimonabant (100 nM) alone and in combination with THC (1 μM) on glutamate levels. $^{**}p < 0.01$ significantly different from control, Rim 100 nM and Rim 100 nM + THC 1 μM. **j** Effect of KYNA (10 nM, 100 nM, and 1 μM) on glutamate levels. **k** Effect of THC (1 μM) alone and in the presence of KYNA (10 and 100 nM) on glutamate levels. $^{**}p < 0.01$ significantly different from control and KYNA 100 nM + THC 1 μM. The results are expressed as percentage of basal glutamate levels, as calculated by the means of the two fractions collected prior to the treatment. Bars represent mean ± SEM ($n = 20$–30). Newman-Keuls test. Rim = Rimonabant

Supplementary Figure S2a). The addition of KYNA (10 nM, 100 nM, and 1 μM) prevented the WIN 55,212-2-induced increase in extracellular glutamate levels (Supplementary Figure S2b, c). KYNA did not influence the effects of lower concentrations of WIN 55,212-2 on glutamate levels (Supplementary Figure S2d–f).

Discussion

The current study yielded several major findings. First, we showed that systemic administration of THC increases extracellular glutamate levels in reward-related brain areas (NAcS, VTA, and mPFC) of freely moving rats and enhances excitability of pyramidal neurons originating in the mPFC and projecting to the NAcS and the VTA, as well as of VTA dopaminergic cells projecting to the NAcS. These effects were prevented by the systemic administration of the KMO inhibitor Ro 61-8048, which enhances the extracellular levels of KYNA, a negative allosteric modulator of the α7nAChRs, in the brain [45]. Second, we found that systemic THC administration decreases extracellular KYNA levels in the NAcS. In the NAcS, both effects—THC-induced increase of glutamate levels and decrease of KYNA levels—were CB1R-dependent. Exposure to THC also increased extracellular glutamate levels in cultured astrocyte preparations, and this effect was prevented by adding exogenous KYNA or the CB1R antagonist rimonabant. Finally, by using RNAscope in situ hybridization, we showed that α7nAChR and CB1R mRNAs are co-localized on rat cortical astrocytes in the mPFC. Together, these results support the hypothesis that activation of reward-related brain circuits by THC might be, at least in part, mediated by increases in glutamate neurotransmission that involve astrocytes.

Although the present results provide compelling evidence for THC-induced increases in extracellular glutamate in dopamine-innervated brain areas, they differ from previous in vitro findings, which showed that cannabinoids *decrease* the release of glutamate in striatal and hippocampal slices, as well as in hippocampal cultures, of rats [12, 58–60]. These results could be reconciled by assuming that, in vivo, the mPFC is a predominant locus of action of the effects of systemically administered THC. In fact, we previously demonstrated that systemically applied THC causes glutamate release in the mPFC [16], explaining both the activation of cortical pyramidal neurons projecting to the NAcS and the VTA, and the glutamate release in these brain areas seen in the present study. Furthermore, our results indicate that the CB1R agonist-induced increase in extracellular glutamate levels in these brain regions in vivo is mainly glia-dependent and not of synaptic origin. Thus, we speculate that systemically applied THC may exert qualitatively distinct, opposing effects on glial and synaptic glutamate, resulting in increased and reduced extracellular levels of the neurotransmitter, respectively. Consequently, the net effect and function of the drug might vary significantly between different brain areas. For example, cannabinoid-induced glutamate deficits in the hippocampus could be related to the deleterious effects of marijuana on memory and learning in humans and animals [3, 61, 62]. In contrast, a preferential *increase* in glutamate release would predominate in reward-related, dopamine-innervated areas and could be mostly responsible for glutamate-dependent dopamine-releasing and reinforcing effects of cannabinoids, as we have hypothesized [45].

We previously showed that systemic administration of the KMO inhibitor Ro 61-8048 in rats rapidly increases KYNA levels in the NAcS and the VTA, and that this effect is associated with a reduction in cannabinoid-induced dopamine release in both areas [45]. Interestingly, Ro 61-8048 also decreased the motivation to self-administer cannabinoids and prevented relapse-like reinstatement of cannabinoid seeking in rats and monkeys [45]. These pharmacological effects of Ro 61-8048 were shown to be dependent on the role of KYNA as a negative allosteric modulator of the α7nAChR [33, 45]. Here we demonstrated that Ro 61-8048 can also effectively block THC-induced glutamate release in the rat NAcS, VTA, and mPFC, and prevent the THC-induced increase in firing rate of pyramidal neurons projecting from the mPFC to the NAcS and VTA. Notably, the effect of THC on glutamate release in the NAcS was also blocked by rimonabant. As activation of CB1Rs on astrocytes stimulates, whereas activation of these receptors on glutamatergic nerve terminals inhibits, glutamate release [13, 63], the present results suggest that more than one mechanism plays a role in this context. Thus, *astrocytic* CB1Rs, as well as α7nAChRs, may be preferentially involved in mediating the effects of THC on glutamate and, secondarily, in the regulation of dopamine release and the reinforcing properties of THC [18–20, 64]. Notably, in the mPFC, THC-induced glutamate release from astrocytes may act in tandem with reduced GABAergic inhibition to activate pyramidal neurons [14, 16].

This possible central role of astrocytes was tested more directly using primary astrocyte cultures of rat cerebral cortex. In this in vitro preparation, exposure to THC was found to concentration-dependently increase extracellular glutamate levels. This effect was prevented by adding either rimonabant or a low (nanomolar) concentration of KYNA to the incubation medium, supporting the hypothesis that the effect is mediated by both CB1Rs and α7nAChRs. As KYNA is synthesized in, and released from, astrocytes [30, 32], the functional relationships between THC, KYNA, and glutamate described in the present study may therefore involve feedback effects of endogenous KYNA on astrocytic α7nAChRs [65, 66].

The connection between cannabinoids, glutamate, and KYNA deserves further consideration in view of the high co-morbidity of cannabis abuse and psychiatric illnesses such as psychotic disorders [67–70]. In fact, cannabis use is significantly more prevalent in persons with psychosis than in the general population [71], and cannabis intoxication can lead to acute transient psychotic episodes and produce short-term exacerbations of pre-existing psychotic symptoms [72–74]. On the other hand, cannabis use can *reduce* negative affective symptoms in patients with an established psychotic disorder [75, 76]. This clinical insight is in agreement with the

observation, in rats, that activation of CB1Rs by the synthetic cannabinoid agonist CP55,940, or by inhibiting the degradation of the endocannabinoid anandamide, *ameliorates* phencyclidine-induced social withdrawal [77], a behavioral correlate of the negative symptoms of schizophrenia [78]. Of note, the improvement of negative symptoms in schizophrenia by THC would be mechanistically in line with an attenuation of glutamate hypofunction and a reduction of the excessive levels of KYNA, which are both seen in the brain of persons with schizophrenia [79–83].

In summary, the present study revealed that both KYNA and glutamate participate in the effects of THC in reward-related brain areas. While the responsible cellular and molecular mechanisms and sequence of the events described in this paper clearly need to be investigated further, astrocytic CB1Rs and α7nAChRs in the mPFC (and possibly also in the NAcS and VTA) appear to play substantive roles in these effects. In addition to resolving apparent inconsistencies between respective studies in rodents and humans regarding the effects of THC on glutamate and dopamine levels [10, 21], future experiments should use genetically modified animals (e.g., conditional knock-out mice lacking CB1R or α7nAChR expression in astrocytes) to elucidate the mechanisms by which CB1Rs control glutamate and KYNA release from astrocytes, and to clarify the specific role of α7nAChRs in this scenario. In turn, these studies could lead to new therapeutic approaches for the treatment of cannabis use disorders and could also provide new tools for dissecting the mechanisms that underlie the therapeutic and abuse-related effects of cannabinoids.

Acknowledgements We thank Dr. Hui-Qiu Wu for performing biochemical analyses in some microdialysis studies and Drs. Ya-Jun Zhang and Xuan (Anna) Li for their kind help with setup of the ISH experiments. We also thank Dr. Yeka Aponte's lab (NIDA, NIH) for allowing us to use the Carl Zeiss confocal microscope for ISH purposes. We dedicate this study to the memory of Dr. Steven R. Goldberg, who passed away on November 25, 2014.

Funding This work was supported in part by the Intramural Research Program of the National Institute on Drug Abuse, National Institutes of Health (MES, PM, GT, SF, LVP, CWS, CWB, SRG, ZJ), USPHS grant P50-MH103222 (to RS), and FAR Grants, University of Ferrara (to LF).

Compliance with Ethical Standards

Experiments were approved by the Animal Care and Use Committees of the Intramural Research Program of NIDA, the University of Cagliari, and the University of Ferrara, respectively, and were carried out in strict accordance with the Guide for the Care and Use of Laboratory Animals (National Research Council, 2003) and the E.C. Regulations for Animal Use in Research (2010/63/EU).

Conflict of Interest MES is currently associated with Institute of Psychopharmacology, Central Institute of Mental Health, Mannheim, Germany. PM is currently associated with Department of Psychiatry and Behavioral Neuroscience, University of Chicago, Chicago, Illinois. The other authors declare that they have no conflict of interest.

References

1. Center for Behavioral Health Statistics and Quality (2015) Results from the 2014 National Survey on Drug Use and Health: volume I. Summary of National Findings. Substance Abuse and Mental Health Services Administration, Rockville, MD.
2. Hall W, Degenhardt L (2008) Cannabis use and the risk of developing a psychotic disorder. World Psychiatry 7(2):68–71
3. Ranganathan M, D'Souza DC (2006) The acute effects of cannabinoids on memory in humans: a review. Psychopharmacology 188(4):425–444
4. Sherif M, Radhakrishnan R, D'Souza DC, Ranganathan M (2016) Human laboratory studies on cannabinoids and psychosis. Biol Psychiatry 79(7):526–538
5. American Psychaitric Association (2013) Diagnostic and statistical manual of mental disorders, 5th edn. American Psychiatric Publishing, Arlington, VA
6. Curran HV, Freeman TP, Mokrysz C, Lewis DA, Morgan CJ, Parsons LH (2016) Keep off the grass? Cannabis, cognition and addiction. Nat Rev Neurosci 17(5):293–306
7. Panlilio LV, Goldberg SR, Justinova Z (2015) Cannabinoid abuse and addiction: clinical and preclinical findings. Clin Pharmacol Ther 97(6):616–627
8. French ED, Dillon K, Wu X (1997) Cannabinoids excite dopamine neurons in the ventral tegmentum and substantia nigra. Neuroreport 8(3):649–652
9. Gessa GL, Melis M, Muntoni AL, Diana M (1998) Cannabinoids activate mesolimbic dopamine neurons by an action on cannabinoid CB1 receptors. Eur J Pharmacol 341(1):39–44
10. Bloomfield MA, Ashok AH, Volkow ND, Howes OD (2016) The effects of Delta9-tetrahydrocannabinol on the dopamine system. Nature 539(7629):369–377
11. Domenici MR, Azad SC, Marsicano G, Schierloh A, Wotjak CT, Dodt HU, Zieglgansberger W, Lutz B et al (2006) Cannabinoid receptor type 1 located on presynaptic terminals of principal neurons in the forebrain controls glutamatergic synaptic transmission. J Neurosci 26(21):5794–5799
12. Shen M, Piser TM, Seybold VS, Thayer SA (1996) Cannabinoid receptor agonists inhibit glutamatergic synaptic transmission in rat hippocampal cultures. J Neurosci 16(14):4322–4334
13. Robbe D, Alonso G, Duchamp F, Bockaert J, Manzoni OJ (2001) Localization and mechanisms of action of cannabinoid receptors at the glutamatergic synapses of the mouse nucleus accumbens. J Neurosci 21(1):109–116
14. Kofalvi A, Rodrigues RJ, Ledent C, Mackie K, Vizi ES, Cunha RA, Sperlagh B (2005) Involvement of cannabinoid receptors in the regulation of neurotransmitter release in the rodent striatum: a combined immunochemical and pharmacological analysis. J Neurosci 25(11):2874–2884
15. Hoffman AF, Riegel AC, Lupica CR (2003) Functional localization of cannabinoid receptors and endogenous cannabinoid production in distinct neuron populations of the hippocampus. Eur J Neurosci 18(3):524–534
16. Pistis M, Ferraro L, Pira L, Flore G, Tanganelli S, Gessa GL, Devoto P (2002) Delta(9)-tetrahydrocannabinol decreases extracellular GABA and increases extracellular glutamate and dopamine levels in the rat prefrontal cortex: an in vivo microdialysis study. Brain Res 948(1–2):155–158
17. Ferraro L, Tomasini MC, Gessa GL, Bebe BW, Tanganelli S, Antonelli T (2001) The cannabinoid receptor agonist WIN 55, 212-2 regulates glutamate transmission in rat cerebral cortex: an in vivo and in vitro study. Cereb Cortex 11(8):728–733
18. Kaiser S, Wonnacott S (2000) Alpha-bungarotoxin-sensitive nicotinic receptors indirectly modulate [(3)H] dopamine release in rat striatal slices via glutamate release. Mol Pharmacol 58(2):312–318

19. Quiroz C, Orru M, Rea W, Ciudad-Roberts A, Yepes G, Britt JP, Ferré S (2016) Local control of extracellular dopamine levels in the medial nucleus accumbens by a glutamatergic projection from the infralimbic cortex. J Neurosci 36(3):851–859
20. Rassoulpour A, Wu HQ, Ferré S, Schwarcz R (2005) Nanomolar concentrations of kynurenic acid reduce extracellular dopamine levels in the striatum. J Neurochem 93(3):762–765
21. Colizzi M, McGuire P, Pertwee RG, Bhattacharyya S (2016) Effect of cannabis on glutamate signalling in the brain: a systematic review of human and animal evidence. Neurosci Biobehav Rev 64: 359–381
22. Justinova Z, Redhi GH, Goldberg SR, Ferré S (2014) Differential effects of presynaptic versus postsynaptic adenosine A2A receptor blockade on Delta9-tetrahydrocannabinol (THC) self-administration in squirrel monkeys. J Neurosci 34(19):6480–6484
23. Metna-Laurent M, Marsicano G (2015) Rising stars: modulation of brain functions by astroglial type-1 cannabinoid receptors. Glia 63(3):353–364
24. Oliveira da Cruz JF, Robin LM, Drago F, Marsicano G, Metna-Laurent M (2016) Astroglial type-1 cannabinoid receptor (CB1): a new player in the tripartite synapse. Neuroscience 323:35–42
25. Navarrete M, Araque A (2008) Endocannabinoids mediate neuron-astrocyte communication. Neuron 57(6):883–893
26. Araque A, Carmignoto G, Haydon PG (2001) Dynamic signaling between astrocytes and neurons. Annu Rev Physiol 63:795–813
27. Nedergaard M, Ransom B, Goldman SA (2003) New roles for astrocytes: redefining the functional architecture of the brain. Trends Neurosci 26(10):523–530
28. Perea G, Navarrete M, Araque A (2009) Tripartite synapses: astrocytes process and control synaptic information. Trends Neurosci 32(8):421–431
29. Volterra A, Meldolesi J (2005) Astrocytes, from brain glue to communication elements: the revolution continues. Nat Rev Neurosci 6(8):626–640
30. Schwarcz R (2016) Kynurenines and glutamate: multiple links and therapeutic implications. Adv Pharmacol 76:13–37
31. Alkondon M, Pereira EF, Yu P, Arruda EZ, Almeida LE, Guidetti P, Fawcett WP, Sapko MT et al (2004) Targeted deletion of the kynurenine aminotransferase ii gene reveals a critical role of endogenous kynurenic acid in the regulation of synaptic transmission via alpha7 nicotinic receptors in the hippocampus. J Neurosci 24(19): 4635–4648
32. Guidetti P, Hoffman GE, Melendez-Ferro M, Albuquerque EX, Schwarcz R (2007) Astrocytic localization of kynurenine aminotransferase II in the rat brain visualized by immunocytochemistry. Glia 55(1):78–92
33. Hilmas C, Pereira EF, Alkondon M, Rassoulpour A, Schwarcz R, Albuquerque EX (2001) The brain metabolite kynurenic acid inhibits alpha7 nicotinic receptor activity and increases non-alpha7 nicotinic receptor expression: physiopathological implications. J Neurosci 21(19):7463–7473
34. Duffy AM, Fitzgerald ML, Chan J, Robinson DC, Milner TA, Mackie K, Pickel VM (2011) Acetylcholine alpha7 nicotinic and dopamine D2 receptors are targeted to many of the same postsynaptic dendrites and astrocytes in the rodent prefrontal cortex. Synapse 65(12):1350–1367
35. Konradsson-Geuken A, Gash CR, Alexander K, Pomerleau F, Huettl P, Gerhardt GA, Bruno JP (2009) Second-by-second analysis of alpha 7 nicotine receptor regulation of glutamate release in the prefrontal cortex of awake rats. Synapse 63(12):1069–1082
36. Marchi M, Risso F, Viola C, Cavazzani P, Raiteri M (2002) Direct evidence that release-stimulating alpha7* nicotinic cholinergic receptors are localized on human and rat brain glutamatergic axon terminals. J Neurochem 80(6):1071–1078
37. Patti L, Raiteri L, Grilli M, Zappettini S, Bonanno G, Marchi M (2007) Evidence that alpha7 nicotinic receptor modulates glutamate release from mouse neocortical gliosomes. Neurochem Int 51(1):1–7
38. Arnaiz-Cot JJ, Gonzalez JC, Sobrado M, Baldelli P, Carbone E, Gandia L, Garcia AG, Hernandez-Guijo JM (2008) Allosteric modulation of alpha 7 nicotinic receptors selectively depolarizes hippocampal interneurons, enhancing spontaneous GABAergic transmission. Eur J Neurosci 27(5):1097–1110
39. Dobelis P, Staley KJ, Cooper DC (2012) Lack of modulation of nicotinic acetylcholine alpha-7 receptor currents by kynurenic acid in adult hippocampal interneurons. PLoS One 7(7):e41108
40. Mok MH, Fricker AC, Weil A, Kew JN (2009) Electrophysiological characterisation of the actions of kynurenic acid at ligand-gated ion channels. Neuropharmacology 57(3):242–249
41. Stone TW (2007) Kynurenic acid blocks nicotinic synaptic transmission to hippocampal interneurons in young rats. Eur J Neurosci 25(9):2656–2665
42. Albuquerque EX, Schwarcz R (2013) Kynurenic acid as an antagonist of alpha7 nicotinic acetylcholine receptors in the brain: facts and challenges. Biochem Pharmacol 85(8):1027–1032
43. Kessler M, Terramani T, Lynch G, Baudry M (1989) A glycine site associated with N-methyl-D-aspartic acid receptors: characterization and identification of a new class of antagonists. J Neurochem 52(4):1319–1328
44. Beggiato S, Tanganelli S, Fuxe K, Antonelli T, Schwarcz R, Ferraro L (2014) Endogenous kynurenic acid regulates extracellular GABA levels in the rat prefrontal cortex. Neuropharmacology 82:11–18
45. Justinova Z, Mascia P, Wu HQ, Secci ME, Redhi GH, Panlilio LV, Scherma M, Barnes C et al (2013) Reducing cannabinoid abuse and preventing relapse by enhancing endogenous brain levels of kynurenic acid. Nat Neurosci 16(11):1652–1661
46. Nagy-Grocz G, Zador F, Dvoracsko S, Bohar Z, Benyhe S, Tomboly C, Pardutz A, Vécsei L (2017) Interactions between the kynurenine and the endocannabinoid system with special emphasis on migraine. Int J Mol Sci 18(8). https://doi.org/10.3390/ijms18081617
47. Solinas M, Tanda G, Justinova Z, Wertheim CE, Yasar S, Piomelli D, Vadivel SK, Makriyannis A et al (2007) The endogenous cannabinoid anandamide produces delta-9-tetrahydrocannabinol-like discriminative and neurochemical effects that are enhanced by inhibition of fatty acid amide hydrolase but not by inhibition of anandamide transport. J Pharmacol Exp Ther 321(1):370–380
48. Wu HQ, Pereira EF, Bruno JP, Pellicciari R, Albuquerque EX, Schwarcz R (2010) The astrocyte-derived alpha7 nicotinic receptor antagonist kynurenic acid controls extracellular glutamate levels in the prefrontal cortex. J Mol Neurosci 40(1–2):204–210
49. Paxinos G, Watson C (2007) The rat brain in stereotaxic coordinates, 6th edn. Academic Press/Elsevier, San Diego
50. Pistis M, Porcu G, Melis M, Diana M, Gessa GL (2001) Effects of cannabinoids on prefrontal neuronal responses to ventral tegmental area stimulation. Eur J Neurosci 14(1):96–102
51. Au-Young SM, Shen H, Yang CR (1999) Medial prefrontal cortical output neurons to the ventral tegmental area (VTA) and their responses to burst-patterned stimulation of the VTA: neuroanatomical and in vivo electrophysiological analyses. Synapse 34(4):245–255
52. Connors BW, Gutnick MJ (1990) Intrinsic firing patterns of diverse neocortical neurons. Trends Neurosci 13(3):99–104
53. Grace AA, Bunney BS (1984) The control of firing pattern in nigral dopamine neurons: burst firing. J Neurosci 4(11):2877–2890
54. Grace AA, Bunney BS (1984) The control of firing pattern in nigral dopamine neurons: single spike firing. J Neurosci 4(11):2866–2876
55. Ungless MA, Magill PJ, Bolam JP (2004) Uniform inhibition of dopamine neurons in the ventral tegmental area by aversive stimuli. Science 303(5666):2040–2042
56. Scuderi C, Valenza M, Stecca C, Esposito G, Carratu MR, Steardo L (2012) Palmitoylethanolamide exerts neuroprotective effects in

mixed neuroglial cultures and organotypic hippocampal slices via peroxisome proliferator-activated receptor-alpha. J Neuroinflammation 9:49
57. Solinas M, Scherma M, Fattore L, Stroik J, Wertheim C, Tanda G, Fratta W, Goldberg SR (2007) Nicotinic alpha 7 receptors as a new target for treatment of cannabis abuse. J Neurosci 27(21):5615–5620
58. Brown TM, Brotchie JM, Fitzjohn SM (2003) Cannabinoids decrease corticostriatal synaptic transmission via an effect on glutamate uptake. J Neurosci 23(35):11073–11077
59. Hoffman AF, Oz M, Yang R, Lichtman AH, Lupica CR (2007) Opposing actions of chronic Delta9-tetrahydrocannabinol and cannabinoid antagonists on hippocampal long-term potentiation. Learn Mem 14(1–2):63–74
60. Takahashi KA, Castillo PE (2006) The CB1 cannabinoid receptor mediates glutamatergic synaptic suppression in the hippocampus. Neuroscience 139(3):795–802
61. Lichtman AH, Martin BR (1996) Delta 9-tetrahydrocannabinol impairs spatial memory through a cannabinoid receptor mechanism. Psychopharmacology 126(2):125–131
62. Wise LE, Thorpe AJ, Lichtman AH (2009) Hippocampal CB(1) receptors mediate the memory impairing effects of Delta(9)-tetrahydrocannabinol. Neuropsychopharmacology 34(9):2072–2080
63. Navarrete M, Araque A (2010) Endocannabinoids potentiate synaptic transmission through stimulation of astrocytes. Neuron 68(1):113–126
64. Grace AA (2006) Disruption of cortical-limbic interaction as a substrate for comorbidity. Neurotox Res 10(2):93–101
65. Sharma G, Vijayaraghavan S (2001) Nicotinic cholinergic signaling in hippocampal astrocytes involves calcium-induced calcium release from intracellular stores. Proc Natl Acad Sci U S A 98(7):4148–4153
66. Wang X, Lippi G, Carlson DM, Berg DK (2013) Activation of alpha7-containing nicotinic receptors on astrocytes triggers AMPA receptor recruitment to glutamatergic synapses. J Neurochemistry 127(5):632–643
67. Volkow ND (2009) Substance use disorders in schizophrenia—clinical implications of comorbidity. Schizophr Bull 35(3):469–472
68. Skosnik PD, Cortes-Briones JA, Hajos M (2015) It's all in the rhythm: the role of cannabinoids in neural oscillations and psychosis. Biol Psychiatry 79:568–577
69. D'Souza DC, Sewell RA, Ranganathan M (2009) Cannabis and psychosis/schizophrenia: human studies. Eur Arch Psychiatry Clin Neurosci 259(7):413–431
70. Wilkinson ST, Radhakrishnan R, D'Souza DC (2014) Impact of cannabis use on the development of psychotic disorders. Curr Addict Rep 1(2):115–128
71. Green B, Young R, Kavanagh D (2005) Cannabis use and misuse prevalence among people with psychosis. Br J Psychiatry 187:306–313
72. Thornicroft G (1990) Cannabis and psychosis. Is there epidemiological evidence for an association? Br J Psychiatry 157:25–33
73. Mathers DC, Ghodse AH (1992) Cannabis and psychotic illness. Br J Psychiatry 161:648–653
74. Hall W, Degenhardt L, Teesson M (2004) Cannabis use and psychotic disorders: an update. Drug Alcohol Rev 23(4):433–443
75. Compton MT, Furman AC, Kaslow NJ (2004) Lower negative symptom scores among cannabis-dependent patients with schizophrenia-spectrum disorders: preliminary evidence from an African American first-episode sample. Schizophr Res 71(1):61–64
76. Dubertret C, Bidard I, Ades J, Gorwood P (2006) Lifetime positive symptoms in patients with schizophrenia and cannabis abuse are partially explained by co-morbid addiction. Schizophr Res 86(1–3):284–290
77. Seillier A, Martinez AA, Giuffrida A (2013) Phencyclidine-induced social withdrawal results from deficient stimulation of cannabinoid CB(1) receptors: implications for schizophrenia. Neuropsychopharmacology 38(9):1816–1824
78. Horan WP, Blanchard JJ, Clark LA, Green MF (2008) Affective traits in schizophrenia and schizotypy. Schizophr Bull 34(5):856–874
79. Erhardt S, Schwieler L, Engberg G (2003) Kynurenic acid and schizophrenia. Adv Exp Med Biol 527:155–165
80. Linderholm KR, Skogh E, Olsson SK, Dahl ML, Holtze M, Engberg G, Samuelsson M, Erhardt S (2012) Increased levels of kynurenine and kynurenic acid in the CSF of patients with schizophrenia. Schizophr Bull 38(3):426–432
81. Nilsson LK, Linderholm KR, Engberg G, Paulson L, Blennow K, Lindstrom LH, Nordin C, Karanti A et al (2005) Elevated levels of kynurenic acid in the cerebrospinal fluid of male patients with schizophrenia. Schizophr Res 80(2–3):315–322
82. Poels EM, Kegeles LS, Kantrowitz JT, Javitt DC, Lieberman JA, Abi-Dargham A, Girgis RR (2014) Glutamatergic abnormalities in schizophrenia: a review of proton MRS findings. Schizophr Res 152(2–3):325–332
83. Schwarcz R, Rassoulpour A, Wu HQ, Medoff D, Tamminga CA, Roberts RC (2001) Increased cortical kynurenate content in schizophrenia. Biol Psychiatry 50(7):521–530